Analysis of MicroRNA Transcriptomes Insights into the miR-148a-3p Inducer of Rumen Development in Goats

Tao Zhong
Sichuan Agricultural University
Cheng Wang
Sichuan Agricultural University
Jiangtao Hu
Sichuan Agricultural University
Xiaoyong Chen
Hebei Agricultural University
Lili Niu (niulili@sicau.edu.cn)
Sichuan agricultural university
Siyuan Zhan
Sichuan Agricultural University
Linjie Wang
Sichuan Agricultural University
Jiaxue Cao
Sichuan Agricultural University
Li Li
Sichuan Agricultural University
Hongping Zhang
Sichuan Agricultural University

Research

Keywords: goat, rumen, RNA sequencing, microRNA, development

Posted Date: July 10th, 2020

DOI: https://doi.org/10.21203/rs.3.rs-40834/v1

Abstract

Background: Rumen is an important digestive organ of ruminant. From fetal to adult stage, the morphology, structure and function of rumen have changed significantly. But the intrinsic genetic regulation is still limited. We previously reported a genome-wide expression profile of miRNAs in prenatal goat rumens. In the present study, we rejoined analyzed the transcriptomes of rumen miRNAs during prenatal (E60 and E135) and postnatal (D30 and D150) stages.

Results: A total of 66 differentially expressed miRNAs (DEMs) were identified in the rumen tissues from D30 and D150 goats. Of these, 17 DEMs were consistently highly expressed in the rumens at the preweaning stages (E60, E135 and D30), while down-regulated at D150. Noteworthy, annotation analysis revealed that the target genes regulated by the DEMs were mainly enriched in MAPK signaling pathway, Jak-STAT signaling pathway and Ras signaling pathway. Interestingly, the expression of miR-148a-3p was significantly high in the embryonic stage and down-regulated at D150. The potential binding sites between miR-148a-3p and *QKI* were predicted by the TargetScan and verified by the dual luciferase report assay. The co-localization of miR-148a-3p and *QKI* was observed not in intestinal tracts but in rumen tissues by *in situ* hybridization. Moreover, the expression of miR-148a-3p in the epithelium was significantly higher than that in the other layers, suggesting that miR-148a-3p involve in the development of rumen epithelial cells by targeting *QKI*. Subsequently, miR-148a-3p inhibitor was found to induce the proliferation of GES-1 cells.

Conclusions: Taken together, these results identified the DEMs involved in the development of rumen and provided an insight into the regulation mechanism of goat rumens during development.

Background

Rumen is the biggest compartment of stomach in adult ruminants, it's special structure plays an important role in the digestion and absorption of nutrients. The development of rumen in goats includes the development of tissue morphology and metabolic function. The rumen wall is thin and slightly transparent, divided into five layers, epithelial layer, lamina propria, submucosa, muscular layer and serous layer [1]. In mature ruminants, the rumen epithelium is involved in many importantly physiological functions, including absorption, transportation, volatile fatty acid (VFA) metabolism, and protection [2]. In addition, a large number of microorganisms in rumen also play a significant role in the processes of digestion and absorption [3]. Up to now, the effects of dietary composition [4] and weaning age [5] on rumen development have been widely investigated, while the roles of microRNAs in rumen development of goats is rarely described.

MicroRNA (miRNA), originally found in *C. elegans*, is a class of non-coding RNA [6]. It mainly regulates the expression of target gene by binding to the sequence of 3'-untranslated region (3'-UTR) [7]. miRNAs can regulate gene expression and participate in the regulation of almost every cellular process [8], such as cell proliferation and differentiation [9], apoptosis and metabolism [10], embryonic development [11]. For instance, it has been reported that overexpression of miR-148a-3p contributed to the proliferation of glomerular cells by targeting *PTEN* in lupus nephritis [12]. Overexpression of miR-148a-3p in fibroblastic osteosarcoma cells increased the number of cells in S phase as well as G2-M phase [13]. In gastric cancer cells, miR-148a might promote gastric cell proliferation by depressing expression of *CDNK1B* [14]. In addition, the *QKI* gene is regulated by a variety of miRNAs, thus affecting many biological processes. miR-214 inhibited angiogenesis via direct targeting of *QKI* and reduced the release of pro-angiogenic growth factor [15]. *QKI* regulated glial cell function by regulating the expression of specific miRNAs [16]. During embryonic development, *QKI* was vital to the myelination and embryogenesis. *QKI* has also been shown to be an anti-apoptotic protein in cardiomyocyte [17].

In our previous study, the expression profile of rumen miRNAs was revealed in the two embryonic stages (E60 and E135) [18]. Here, we investigated the DEMs identified in the pre-weaning and post-weaning stages (D30 and D150) and rejoined analyzed the RNA sequencing data. Furthermore, we identified miR-148a-3p regulated the expression of *QKI* by directly targeting 3'-UTR of *QKI*. Inhibition of the expression of miR-148a-3p could significantly improve the proliferation capacity of GES-1 cells, suggesting that miR-148a-3p may be involved in the process of rumen development in goats.

Materials And Methods

Experimental Animals and rumen tissue collection

The goats used in this experiment were provided by the Jianzhou Da'er Goat Breeding Center (Sichuan, China). Rumen tissues were collected from goats at the four different periods (E60, E135, D30 and D150) to perform the high-throughput sequencing. The rumen tissues were frozen in liquid nitrogen immediately after collection, and then stored at -80 °C. All experiments involving animals was conducted according to the Regulations for the Administration of Affairs Concerning Experimental Animals (Ministry of Science and Technology, China, revised in June 2004).

RNA Isolation, Library Construction, and Sequencing

Total RNA was extracted from rumen tissues using TRIzol, according to the manufacturer's instructions. The purity, concentration, and quality of RNA were determined by Nanodrop 2000 spectrophotometer, Qubit 3.0 Fluorometer, and Agilent 2100 Bioanalyzer, respectively. Libraries were constructed with RNA using the TruSeq small RNA Sample Pre Kit (Illumina, San Diego, USA). Finally, the libraries were sequenced on Illumina Hiseq 2500 platform.

miRNAs Data Analyses and qPCR validation

Two data sets, the new obtained raw data (D30 and D150) and our previous data (E60 and E135) were jointly analyzed in the present study. The analyses procedures of miRNA identification, expression, function and targets prediction were performed according to the methods [19-23]. DEMs were identified using the criteria of fold change ≥ 1 and *P*-value ≤ 0.01. To verify the high-throughput sequencing data, we randomly selected 8 miRNAs from the identified DEMs by qRT-PCR. Total RNA (5 μg) was reverse transcribed into cDNA using the Mir-XTM miRNA First-Strand Synthesis Kit (TaKaRa, Dalian, China). The primer sequences for qRT-PCR are listed in Additional file 1: Table S1. qRT-PCR was performed using the SYBR PrimeScript miRNA RT-PCR Kit (Takara) on a CFX

Connect Real-Time PCR Detection System (Bio-Rad Laboratories, Singapore). Briefly, a volume of 10 μL including 5 μL of SYBR Green Real Time PCR Master Mix (TaKaRa), 0.2 μL each of forward and reverse primer, 3.8 μL of RNase-Free ddH_2O, and 0.8 μL of cDNA. qPCR reactions were performed using the following condition: 95.0 °C for 30 sec, and 40 cycles of 95.0 °C for 5 sec, Tm for 30 sec. U6 was used as reference gene. The expression level of miRNA was calculated with the $2^{-\Delta\Delta CT}$ method [24]. All samples were run in triplicate.

Expression vector construction

The putative binding sites of miR-148a-3p and *QKI* 3'-UTR were predicted the TargetScan website (www.targetscan.org). The wild-type (wt) 3'-UTR of *QKI* was amplified by PCR. Sequences of the primers used in vector construction assays are listed in Supplemental Table 1. PCR amplification system contained a 30 μL volume including 2× Master Mix Taq, forward and reverse primers 2 μL, cDNA 1 μL and ddH_2O 12 μL. The reaction cycler conditions: 95.0 °C for 5 min; 95.0 °C for 30 sec, Tm for 30 sec, 72 °C for 30 sec, 35 cycles; 72 °C 5 min. The amplified product and the psiCHECK-2 vector (Promega, USA) were digested. The digestion system was placed at 37 °C for 2 h. The digestion products were recovered and incubated at 16 °C overnight using T4 ligase. The DH5α (TIANGEN, Beijing, China) competent cells (50 μL) were added to the ligation, culled from a single colony, identified and verified by sequencing. The psi-CHECK2 plasmid containing the mutant type (mut) 3'-UTR of *QKI* was obtained from GeneCreate Biological Engineering (Wuhan, China).

Cell culture, transfection and expression detection

HEK293T cells were used to detect luciferase activity, and GES-1 (BNCC, Beijing, China) cells were used to detect the effect of miR-148a-3p on cell proliferation. Cells were maintained in DMEM supplied with 10% FBS at a 37 °C incubator containing 5% CO_2. Lipofectamine™ 2000 (Invitrogen, Carlsbad, CA, USA) was used for cell transfection following the manufacturer's procedure. GES-1 cells were transfected with miR-148a-3p mimics, miR-148a-3p inhibitor, miR-148a-3p-NC, *QKI* siRNA or *QKI*-NC at the concentration of 50 nM, respectively. miR-148a-3p mimics and mimic control were chemically synthesized by Ribo Bio Co. Ltd (Guangzhou, China). The expression levels of miR-148a-3p and *QKI* isoforms in each group were detected by qPCR at 48 h post-transfection. *QKI5 QKI6* and *QKI7* primers are designed in their corresponding specific sequence positions (Additional file 2: Figure S1).

Luciferase Reporter Assay

For luciferase reporter assay, HEK293T cells were were co-transfected with miR-148a-3p mimics (or miR-148a-3p NC) and wt-QKI-3'-UTR plasmids (or mut-QKI-3'-UTR plasmids) using Lipofectamine 2000. After transfection 48 h, the luciferase activities were measured on a GloMax® 96 Microplate Luminometer (Promega) by the TransDetect Double-Luciferase Reporter Assay Kit (TaKaRa).

Cell Proliferation Assays

The GES-1 cells was used to study cell proliferation by the Cell Counting kit-8 (Dojindo, Shanghai, China). The GES-1 cells were seeded into 96-well plates at a density of 1×10^4 cells per well determined by the Corning Cell Counter (NY, USA). After transfection of the miR-148a-3p mimics or the miR-148a-3p-NC, the cells were cultured for 4, 24, 48 and 72 h. Then, the absorbance of cells was measured with a wavelength of 450 nm using a micro-plate reader (Analytik Jena AG, Germany).

Dual-color Fluorescence in situ Hybridization

Briefly, tissue sections were deparaffinized, dehydrated, and incubated in room temperature for 15 min, digested in pepsin solution for 3-30 min at 37°C. Denaturation, hybridization, and post-hybridization washings were carried out by following the manufacturer's instructions. After DAPI staining for 10 min, wash with 0.5 × SSC for 15 min; wash with 0.2 × SSC for 15 min at 37 °C. miR-148a-3p was labeled with red, while *QKI* was labeled with green. Images were captured by an Olympus BX51T fluorescence microscope (Olympus, Japan) and analyzed by the Image-Pro Plus software (Media Cybernetics, USA).

Statistical analyses

Statistical analyses were conducted using SPSS 20.0 software. Data were analyzed by one-way analysis of variance (ANOVA). The differences between the groups were analyzed using Student's t-test and multiple comparison tests. The differences between the means were considered statistically significant when $P < 0.05$.

Results

miRNAs expression profile and DEMs in goat rumens

Twelve rumen samples representing four developmental stages (E60, E135, D30 and D150) were performed RNA-sequencing and jointly analyzed to profile the miRNAs expression pattern of rumen tissues in this study. An average of 18.59 million single-end clean reads was generated, and approximately 50.6% mapped to the goat reference genome ARS1 (Additional file 3: Table S2). A total of 1,488 miRNAs were identified in the rumen samples, including 431 known miRNAs and 1,057 novel miRNAs (Additional file 4: Table S3). The top-10 miRNAs are listed in Table 1. Seven miRNAs (miR-143-3p, let-7i-5p, miR-148a-3p, let-7f-5p, miR-21-5p, miR-26a-5p and let-7g-5p) were consistently highly expressed in the rumen tissues at the four stages.

In postnatal period, 35 up-regulated DEMs and 31 down-regulated DEMs were observed between the rumens at D30 and D150 (Fig. 1a, Additional file 5: Table S4). The hierarchical cluster of these 66 DEMs was shown in Fig. 1b. Interestingly, there were comparable DEMs in the pairwise E60 vs. D30 (27 up-regulated and 12 down-regulated) and E135 vs. D30 (19 up-regulated and 25 down-regulated) comparisons, while in the pairwise E60 vs. D150 (53 up-regulated and 29 down-regulated) and E135 vs. D150 (67 up-regulated and 44 down-regulated) the number of DEMs was markedly increased (Additional file 6: Figure S2). Venn

diagrams (Fig. 1c) showed the DEMs in each comparison of all the stages. In general, the number of DEMs was increased followed by the development of goat rumen, especially for the functional transition of the rumen epidermal layer from maternal glucose dependence in the fetal period to utilization of short chain fatty acids (SCFA) in feed after weaning. The expression patterns of the selected DEMs were verified by qPCR and consistent with the tendency of the small RNA-sequencing data (Fig. 2).

GO and KEGG pathway analyses of putative target genes

To elucidate the biological roles on development of rumens, the target genes of the DEMs were subjected to Gene Ontology (GO) analysis. Fifty-two GO terms were identified, including 24 biological processes, 17 cellular components, and 11 molecular functions (Fig. 3a). The analysis of biological process showed that the most genes were involved in cellular process and biological regulation. On the molecular function level, GO terms were mainly involved in binding and catalytic activity. On the cellular component level genes were mainly related to organelle and cell part. Meanwhile, the biological pathways involved in rumen development were revealed by the Kyoto Encyclopedia of Genes and Genomes (KEGG) analysis based on all the DEMs. In total, 188 signaling pathways were considered as significantly enriched (Additional file 7: Table S5), and involved in MAPK signaling pathway, Rap1 signaling pathway, Ras signaling pathway and Jak-STAT signaling pathway, which were linked to cell proliferation (Fig. 3b). In addition, six specific GO terms and thirty-five KEGG categories were revealed between embryonic and post-weaning stages (Additional file 8: Table S6). Furthermore, eight KEGG pathways were identified between pre-weaning and post-weaning periods, which enriched in tryptophan metabolism and glycosaminoglycan biosynthesis (Additional file 8: Table S6).

Candidate miR-148a-3p expression and target gene analysis

The expression pattern of miR-148a-3p in the rumens was shown in Table 1, representing a significant high expression level in pre-weaning stages (E60, E135 and D30). A significant low expression was observed in the rumen at post-weaning period (D150), indicating miR-148a-3p acts an especially important role in the development of rumen epithelium cells.

The potential target genes (Additional file 9: Table S7) of miR-148a-3p were estimated by the Targetscan analysis. As for correlation of expression of miR-148a-3p and *QKI* was significantly highest, *QKI* was selected as the target gene to be further investigated. The binding sites of *QKI* 3'-UTR are highly conserved in various species, including goat, sheep and cow. The predicted minimum free energy of miR-148a-3p and *QKI* mRNA was found to be -22.9 kcal/mol (Fig. 4a). The recombinant plasmid was constructed by the length of 257 bp from the 3'-UTR of *QKI* and an approximate 6.2 KB fragment of psiCHECK-2 vector (Fig. 4b). Furthermore, we employed a luciferase reporter assay to identify the binding of miR-148a-3p and 3'-UTR of *QKI*. We constructed luciferase reporter plasmids containing wild-type and mutant 3'-UTR of *QKI* (Fig. 4c), and then co-transfected with miR-148a-3p mimics or negative control in HEK293T cells. The luciferase reporter activity of co-transfected miR-148a-3p mimics and wild type was significantly lower than that of co-transfected miR-148a-3p negative control and wild type (Fig. 4d, $P < 0.01$). The luciferase reporter activity of co-transfected miR-148a-3p mimics and mutant was not significantly different from that of co-transfected miR-148a-3p negative control and mutant. In addition, the luciferase reporter activity of co-transfected miR-148a-3p mimics and wild-type mimics was significantly lower than that of co-transfected miR-148a-3p mimics and mutant mimics ($P < 0.01$). These results indicated that miR-148a-3p could bind to the 3'-UTR of *QKI*, thereby inhibiting the expression of *QKI*.

Co-localization of miR-148a-3p and QKI in goat digestive tissues

The co-localization of miR-148a-3p and *QKI* in rumen, reticulum, omasum and abomasum was performed by double-color fluorescence *in situ* hybridization (Fig. 5). The signal locations of miR-148a-3p and *QKI* were consistent, and miR-148a-3p and *QKI* were expressed in all layers of the gastric wall, but significantly higher in the epithelial layer than in other layers. Therefore, we speculated that miR-148a-3p play an important role in the development of rumen epithelial cells by targeting *QKI*. In order to further explore the potential functions of miR-148a-3p and *QKI* in intestinal tract, we also investigated their co-localization in duodenum, jejunum, ileum and colon (Additional file 10: Figure S3). The results showed that miR-148a-3p and *QKI* were located inconsistently in many structures, and the expression levels of miR-148a-3p and *QKI* in various types of intestinal tract were relatively low. In duodenal sections, miR-148a-3p was higher in the muscularis than that in the villus, while *QKI* was highly expressed in the villus than that in the muscularis. The signal intensity of miR-148a-3p and *QKI* on the vascular wall of colon was significantly higher than that of other structures. Thus, miR-148a-3p did not bind *QKI* in intestinal tract, while co-localization on the vascular wall suggested that miR-148a-3p may be involved in some of certain functions.

miR-148a-3p affects cell proliferation by targeting QKI

To investigate the effect of miR-148a-3p on cell proliferation, we co-transfected miR-148a-3p mimics, inhibitor or negative control, and *QKI* siRNA or negative control within GES-1 cells, respectively. As shown in Fig. 6, expression of miR-148a-3p was determined by qRT-PCR after transfection, miR-148a-3p expression was significantly higher than that of the negative control (Fig. 6a). proliferation of GES-1 cells was then assessed at 4 h, 24 h (D1), 48 h (D2) and 72 h (D3) by the CCK8 kit, there was no significant difference in cell proliferation between the GES-1 cells overexpressing miR-148a-3p and the negative control (Fig. 6b). As shown in Fig. 5c, the expression levels of *QKI5*, *QKI6* and *QKI7* in the GES-1 cells overexpressing miR-148a-3p were all down-regulated, and the expression of *QKI5* and *QKI6* was significant down-regulation. Conversely, expression of *QKI5*, *QKI6* and *QKI7* was significantly down-regulated in GES-1 cells transfected with *QKI* siRNA (Fig. 6e). However, there was no significant effect on the proliferation of GES-1 cells (Fig. 6d). Taken together, these data suggest that the endogenous high expression of miR-148a-3p in GES-1 cells may be the reason why overexpression of miR-148a-3p has no significant effect on cell proliferation, while *QKI*, as the target gene of miR-148a-3p, is inhibited in cells with overexpression of miR-148a-3p, so silencing of *QKI* also has no significant effect on cell proliferation.

Intriguingly, the expression of miR-148a-3p was significantly deceased after transfection with miR-148a-3p inhibitor (Fig. 6f). As shown in Fig. 6g, the proliferation of GES-1 cells was significantly increased after 48 h transfection. Compared to negative control, expression level of *QKI5* were slightly up-

regulated, while the expressions of *QKI6* were significantly down-regulated (Fig. 6h). These data suggest that miR-148a-3p could inhibit the expression of *QKI5* by binding to its 3'-UTR. Furthermore, inhibition of miR-148a-3p expression could promote the proliferation ability of GES-1 cells.

Discussion

Expression profiles of goat rumens during pre- and post-weaning periods

In the present study, we mainly focused on the expression characteristics of genome-wide microRNAs involved in rumen development and their potentially affects especially on the functional transition of the rumen epidermal layer in goats. Seven highly expressed miRNAs mainly involving in cell proliferation, growth and apoptosis were identified at the four tested periods. Among them, miR-143-3p has been verified to be related with the regeneration of skeletal muscle cells by targeting *IGFBP5* [25], and it could target the CTGF and inhibit the Akt/mTOR signaling pathway to regulate the proliferation and apoptosis of fibroblasts [26]. miR-21-5p and miR-26a-5p have also been shown to be associated with the proliferation of melanoma and hepatocellular carcinoma cells, respectively [27, 28]. As for the members of let-7, expressions of let-7i-5p, let-7f-5p and let-7g-5p have been revealed to regulate the regeneration rate of liver in mice [29].

Compared with the rumens from post-weaning period (D150), a similarity number of DEMs (82 in E60 and 111 in E135) were detected the rumens at prenatal stages (Additional file 6: Figure S2). It was notable that the rumen function was absorption maternal glucose in embryonic stage, while solely obtain energy from SCFA in feed after weaning. From fetal to birth and adult stage, the morphology, structure and function of rumen have significantly changed, especially the surface area of the rumen papillae of goats under supplementary feeding significantly increased during the pre- and post-weaning periods [30]. 66 DEMs were observed between the rumens at D30 and D150 (Fig. 1a). We previously reported that miRNAs expression in embryonic rumens and less number of DEMs (22 up-regulated and 20 down-regulated) was identified between E60 and E135 [18].

Histomorphological analyses have found that rumen development in cattle [31] and sheep [32] were slightly faster than that in goats during embryonic period. During weaning, the length and surface area of the rumen papillae of goats and calves increased, and rumen development significantly changed [33, 34]. Accompanied by the development of rumen size, rumen papillae and muscular tissues, gene expression were also remarkably altered though transcriptional and post-transcriptional regulation. Plenty of differential expressed genes (DEGs) have been identified in cattle between pre- and post-weaning [2, 35, 36]. During weaning, the DEGs in calf rumen epithelium were mainly involved in the processes of lipid metabolism, cell morphology, growth and proliferation, molecular transport [2]. Later, more DEGs (4,104) were revealed between the pre- and the post-weaning periods in bovine rumen and several highly DEGs with immune functions (*LY6D*, MUC1, *EMB* and *EYA2*) were pointed out. Similarity, immunity and lipid metabolism were also significantly enriched for DE genes in the rumen [35]. Subsequently, 122 DEMs were identified from 260 known and 35 novel miRNAs in the same rumen tissues. Among them, six miRNAs (miR-143, miR-29b, miR-145, miR-493, miR-26a and miR-199) were identified as the key regulators of rumen development in cattle [36]. However, the studies about miRNAs in goat rumens still limited.

miRNAs related with the pathways involved in rumen development

With regard to biological functions of the target genes of DEMs, four relevant pathways were enriched significantly in goat rumens, including the MAPK signaling pathway, Jak-STAT signaling pathway, Rap1 signaling pathway, Ras signaling pathway and PI3K-Akt signaling pathway (Fig. 2b). Several factors could effect cell proliferation and differentiation mediated by the epidermal growth factor receptor (EGFR) with respond to EGF and transmembrane transforming growth factor (TGF) through the MAPK signaling pathway [37], it promoted the growth of gastric epithelium during development and the renewal of the gastric tissue [38]. It has been shown that inhibition of Jak-STAT3 signaling pathway could inhibit cell proliferation in gastric cancer cells [39]. Ras signaling was a downstream pathway of EGFR and played an important role in the cell fate and proliferation of intestinal epithelial cells [40]. In addition, phosphorylation of PI3K-Akt signaling pathway can promote ghrelin-mediated intestinal cell proliferation [41]. These findings indicated that epithelial cell proliferation during rumen development is closely related to MAPK signaling pathway, Ras signaling pathway and PI3K-Akt signaling pathway.

Compared with prenatal rumens (E60 and E135), the differently enriched pathways at the post-weaning stage (D150) were mainly clustered into carbohydrate digestion and absorption, vitamin digestion and absorption, adherens junction, gap junction, amino acid metabolism (Additional file 8: Table S6). Subsequently, the specific pathways including tryptophan and metabolism, ether lipid metabolism and glycosaminoglycan biosynthesis were revealed in comparison of pre- and post-weaning rumens (D30 and D150). During the processes of rumen development, the histomorphology changes and functional transitions of rumen should be followed by gene regulation [42]. These results indicated that some DEMs may be involved in epithelial cell junctions, digestion and metabolism of nutrients.

To date, many investigations have focused on the molecular mechanism of rumen epithelial cell proliferation and related transporter regulatory pathways, such as insulin-like growth factor (IGF) and epidermal growth factor (EGF) involved in the regulation of glucose transport, NHE, MCTs and GPR involved in the transport of SCFA in rumen epithelial cells [43, 44]. With respect to other external effects, diet composition and nutrient level can affect rumen development, and the expression of epithelial cell genes can also affect gastrointestinal development. Malmuthuge and colleagues demonstrated that the VFAs produced by microbiota could stimulate processes of rumen tissue metabolism and epithelium development via interacting with the host transcriptome and microRNAome. Approximately half of miRNAs and over 25% of mRNAs were correlated with the diversities of VFAs in neonatal calves [45]. In addition, ratio of non-fibrous carbohydrate/neutral detergent fiber (NFC/NDF) in diet could affect the the length and width of rumen papillae. One differently expressed bta-miR-128 induced by NFC/NDF was found to regulate the rumen development via regulating *PPARG* and *SLC16A1* genes [46]. Moreover, in grass- and grain-fed cattle could also resulted in alternations of miRNA expression potentially influencing rumen function, as well as mRNA expression and DNA methylation [47].

miR-148a-3p functions in proliferation, differentiation and apoptosis

In the current study, we have found that miRNA-148a-3p was highly expressed in rumen tissues, especially in D30 (2-fold), while its underlying regulatory mechanism in rumen development remains unclear. FISH results (Fig. 6) demonstrated that miR-148a-3p and *QKI* were co-expressed in rumen, reticulum, omasum and bomasum, compared with in other gastrointestinal tract samples, miR-148a-3p and *QKI* are expressed in different locations (Additional file 10: Figure S3). Furthermore, a high correlation of miR-148a-3p and *QKI* expression was found at all the four periods (Additional file 9: Table S7). As revealed in GES-1 cells, miR-148a-3p suppressed the cell proliferation by regulating *QKI*, suggesting that a similarity effects on the rumen epithelial cells.

A previous study has revealed that miR-148a-3p was significantly up-regulated during fetal liver development, and its target gene also participated in the differentiation process of liver cells [48]. miR-148a-3p could induce hepatocytic differentiation by inhibiting the IKKα/NUMB/NOTCH signaling pathway [49]. In domestic animals, miR-148a-3p was highly expressed in fetal bovine skeletal muscle, but decreased in the growing myocytes. It was found that the overexpression of miR-148a-3p could inhibit the proliferation of myocytes and promote the proliferation of myocytes after interference [50]. In rabbits, miR-148a-3p is not only highly expressed in white adipose tissue at early growth stage, but also gradually increased in the differentiation process of preadipocytes cultured in vitro [51]. In pigs, miR-148a-3p was always highly expressed during the development of skeletal muscle, which was speculated to be related to the proliferation, generation and apoptosis of muscle cells [52].

Here, *QKI* was confirmed to be a target gene of miR-148a-3p in goat rumens. *QKI* is a kind of RNA binding protein, which is a member of RNA signal transduction and activation family and plays an important role in mammalian embryo development. *QKI* protein has a maxi-KH domain, which is transcriptionally controlled by *QKI*-RNA recognition element CUAAC sequence, which is involved in many RNA metabolic processes, and has a target regulatory role in the localization, translation, transport and stability of mRNA [53]. The main subtypes of *QKI* are *QKI5*, *QKI6* and *QKI7*, in which *QKI5* mainly exists in the nucleus, *QKI6* is distributed in all parts of the cell, and *QKI7* mainly exists in the cytoplasm. The expression of *QKI* was regulated by various miRNAs, which affected its biological functions. For example, miR-214 can target and regulate the expression of *QKI* and participate in the differentiation of vascular smooth muscle cells [54]. miR-148a-3p could affect the proliferation of cancer cells by targeting *QKI5* [55]. In addition, *QKI* can also act on miRNAs precursor and feedback regulate miRNAs expression [16].

Previous studies reported that the expression of miR-148a-3p was affected by methylation. The expression of *QKI* was also affected by the methylation level of its promoter region, which contained CpG islands in the upstream region of pre-miR-148a-3p [56]. Meanwhile, miR-148a-3p also regulated the expression of *DNMT1* and affected the physiological processes of different cells [57-59]. The binding site of miR-148a-3p was also confirmed to be existance in the 3'-UTR of *DNMT1*. Thus, It is speculated that the expression of miR-148a-3p should be regulated by epigenetics [60]. In this study, we found that the expression of miR-148a-3p was significantly different in the rumen tissues between embryonic stage and after weaning. miR-148a-3p may affect cell proliferation by binding to *QKI5* 3'-UTR and inhibiting its expression. Therefore, during rumen development, DNA methylation whether involve in and how to regulate the expression of miR-148a-3p and *QKI* remains to be further studied.

Conclusion

In summary, genome-wide expression profile of miRNAs and specific pathways involved in the development of rumen were identified in goats. FISH and luciferase experiments verified that *QKI* is a potential target gene of miR-148a-3p. Furthermore, suppression of miR-148a-3p could induced the proliferation of GES-1 cells. Our results indicate that miR-148a-3p may be an inducer of rumen development in goats by targeting *QKI*.

Abbreviations

DEMs: differentially expressed miRNAs; **VF:** volatile fatty acid; **3'-UTR:** 3'-untranslated region; **SCFA:** short chain fatty acids; **GO:** Gene ontology; **KEGG:** Kyoto Encyclopedia of Genes and Genomes; **DEGs:** differential expressed genes; **EGFR:** epidermal growth factor receptor; **EGF:** epidermal growth factor; **TGF:** transmembrane transforming growth factor; **IGF:** insulin-like growth factor; **NFC/NDF:** non-fibrous carbohydrate/neutral detergent fiber.

Declarations

Ethics approval and consent to participate

The protocol for collecting ruminal biopsies was approved by the Institutional Animal Care and Use Committee of the College of Animal Science and Technology of Sichuan Agricultural University, Sichuan, China, under the permit of No. DKY-B20131403.

Consent for publication

Not applicable.

Availability of data and material

Goat rumen RNA-Seq data are accessible at SRA database (PRJNA596079).

Competing interests

The authors declare no conflicts of interests.

Funding

This work was supported by the National Key Research and Development Program of China (2018YFD0502002) and the Chinese Domestic Animal Germplasm Resources Infrastructure.

Authors' contributions

TZ and LLN conceived and designed the experiments. CW and JTH performed the experiments. SYZ analyzed the data. LJW, JZG, LL, and HPZ participated in sample collection. HPZ, LLN and TZ contributed reagents/materials. CW, LLN and TZ wrote the manuscript.

Acknowledgements

We are grateful to Qianjun Zhao from CAAS for processing data and the native English-speaking scientists of “American Journal Experts (Durham, North Carolina, USA)” for proofreading the article.

References

1. Garcia A, Masot J, Franco A, Gazquez A, Redondo E. Histomorphometric and immunohistochemical study of the goat rumen during prenatal development. Anat Rec. 2012;295(5):776-85.
2. Connor EE, Baldwin RLt, Li CJ, Li RW, Chung H. Gene expression in bovine rumen epithelium during weaning identifies molecular regulators of rumen development and growth. Func Integr Genomics. 2013; 13(1):133-42.
3. Liu K, Xu Q, Wang L, Wang J, Guo W, Zhou M. The impact of diet on the composition and relative abundance of rumen microbes in goat. Asian-Australas J Anim Sci. 2017; 30(4):531-37.
4. Jing XP, Peng QH, Hu R, Zou HW, Wang HZ, Yu XQ, et al. Dietary supplements during the cold season increase rumen microbial abundance and improve rumen epithelium development in Tibetan sheep. J Anim Sci. 2018; 96(1):293-305.
5. Carballo OC, Khan MA, Knol FW, Lewis SJ, Stevens DR, Laven RA, et al. Impact of weaning age on rumen development in artificially reared lambs1. J Anim Sci. 2019; 97(8):3498-510.
6. Lee RC, Feinbaum RL, Ambros V. The C. elegans heterochronic gene lin-4 encodes small RNAs with antisense complementarity to lin-14. Cell. 1993; 75(5):843-54.
7. Shukla GC, Singh J, Barik S. MicroRNAs: Processing, Maturation, Target Recognition and Regulatory Functions. Mol Cell Pharmacol. 2011; 3(3):83-92.
8. Krol J, Loedige I, Filipowicz W. The widespread regulation of microRNA biogenesis, function and decay. Nat Rev Genet. 2010; 11(9):597-610.
9. Bartel DP. MicroRNAs: genomics, biogenesis, mechanism, and function. Cell. 2004; 116(2):281-97.
10. Kloosterman WP, Plasterk RH. The diverse functions of microRNAs in animal development and disease. Dev Cell. 2006; 11(4):441-50.
11. Wienholds E, Kloosterman WP, Miska E, Alvarez-Saavedra E, Berezikov E, de Bruijn E, et al. MicroRNA expression in zebrafish embryonic development. Science. 2005; 309(5732):310-11.
12. Qingjuan L, Xiaojuan F, Wei Z, Chao W, Pengpeng K, Hongbo L, et al. miR-148a-3p overexpression contributes to glomerular cell proliferation by targeting PTEN in lupus nephritis. Am J Physiol Cell Physiol. 2016, 310(6):C470-8.
13. Bhattacharya S, Chalk AM, Ng AJ, Martin TJ, Zannettino AC, Purton LE, et al. Increased miR-155-5p and reduced miR-148a-3p contribute to the suppression of osteosarcoma cell death. Oncogene. 2016; 35(40):5282-94.
14. Guo SL, Peng Z, Yang X, Fan KJ, Ye H, Li ZH, et al. miR-148a promoted cell proliferation by targeting p27 in gastric cancer cells. Int J Biol Sci. 2011; 7(5):567-74.
15. Mil AV, Grundmann S, Goumans MJ, Lei Z, Oerlemans MI, Jaksani S, et al. MicroRNA-214 inhibits angiogenesis by targeting Quaking and reducing angiogenic growth factor release. Cardiovasc Res. 2012; 93(4):655-65.
16. Wang Y, Vogel G, Yu Z, Richard S. The QKI-5 and QKI-6 RNA binding proteins regulate the expression of microRNA 7 in glial cells. Mol Cell Biol. 2013; 33(6):1233-43.
17. Guo W, Shi X, Liu A, Yang G, Yu F, Zheng Q, et al. RNA binding protein QKI inhibits the ischemia/reperfusion-induced apoptosis in neonatal cardiomyocytes. Cell Physiol Biochem. 2011; 28(4):593-602.
18. Zhong T, Hu J, Xiao P, Zhan S, Wang L, Guo J, et al. Identification and Characterization of MicroRNAs in the Goat (Capra hircus) Rumen during Embryonic Development. Front Genet. 2017; 8:163.
19. Ashburner M, Ball CA, Blake JA, Botstein D, Butler H, Cherry JM, et al. Gene ontology: tool for the unification of biology. The Gene Ontology Consortium. Nat Genet. 2000; 25(1):25-9.
20. Betel D, Wilson M, Gabow A, Marks DS, Sander C: The microRNA.org resource: targets and expression. Nucleic Acids Res. 2008; 36:D149-53.
21. Friedlander MR, Mackowiak SD, Li N, Chen W, Rajewsky N. miRDeep2 accurately identifies known and hundreds of novel microRNA genes in seven animal clades. Nucleic Acids Res. 2012; 40(1):37-52.
22. Kanehisa M, Goto S, Kawashima S, Okuno Y, Hattori M. The KEGG resource for deciphering the genome. Nucleic Acids Res. 2004; 32:D277-80.
23. Love MI, Huber W, Anders S. Moderated estimation of fold change and dispersion for RNA-seq data with DESeq2. Genome Biol. 2014; 15(12):550.
24. Schmittgen TD, Lee EJ, Jiang J, Sarkar A, Yang L, Elton TS, et al. Real-time PCR quantification of precursor and mature microRNA. Methods. 2008, 44(1):31-8.
25. Soriano-Arroquia A, McCormick R, Molloy AP, McArdle A, Goljanek-Whysall K. Age-related changes in miR-143-3p:Igfbp5 interactions affect muscle regeneration. Aging cell. 2016; 15(2):361-9.

26. Mu S, Kang B, Zeng W, Sun Y, Yang F. MicroRNA-143-3p inhibits hyperplastic scar formation by targeting connective tissue growth factor CTGF/CCN2 via the Akt/mTOR pathway. Mol Cell Biochem. 2016; 416(1-2):99-108.
27. Yang Z, Liao B, Xiang X, Ke S. miR-21-5p promotes cell proliferation and G1/S transition in melanoma by targeting CDKN2C. FEBS Open Bio. 2020; 10(5):752-60.
28. Yuan YL, Yu H, Mu SM, Dong YD, Li Y. MiR-26a-5p Inhibits Cell Proliferation and Enhances Doxorubicin Sensitivity in HCC Cells via Targeting AURKA. Technol Cancer Res Treat. 2019; 18:1533033819851833.
29. Dkhil MA, Al-Quraishy SA, Abdel-Baki AS, Delic D, Wunderlich F. Differential miRNA Expression in the Liver of Balb/c Mice Protected by Vaccination during Crisis of Plasmodium chabaudi Blood-Stage Malaria. Front Microbiol. 2016; 7:2155.
30. Htoo NN, Zeshan B, Khaing AT, Kyaw T, Woldegiorgis EA, Khan MAKG. Creep Feeding Supplemented with Roughages Improve Rumen Morphology in Pre-Weaning Goat Kids. Pak J Zool. 2018; 50(2).
31. Vivo JM, Robina A, Regodon S, Guillen MT, Franco A, Mayoral AI. Histogenetic evolution of bovine gastric compartments during the prenatal period. Histol Histopathol. 1990; 5(4):461-76.
32. Franco A, Regodon S, Robina A, Redondo E. Histomorphometric analysis of the rumen of sheep during development. Am J Vet Res. 1992; 53(7):1209-17.
33. Jiao J, Li X, Beauchemin KA, Tan Z, Tang S, Zhou C. Rumen development process in goats as affected by supplemental feeding v. grazing: age-related anatomic development, functional achievement and microbial colonisation. Br J Nutr. 2015; 113(6):888-900.
34. Roth BA, Keil NM, Gygax L, Hillmann E. Influence of weaning method on health status and rumen development in dairy calves. J Dairy Sci. 2009; 92(2):645-56.
35. Ibeagha-Awemu EM, Do DN, Dudemaine PL, Fomenky BE, Bissonnette N. Integration of lncRNA and mRNA Transcriptome Analyses Reveals Genes and Pathways Potentially Involved in Calf Intestinal Growth and Development during the Early Weeks of Life. Genes (Basel). 2018; 9(3):142
36. Do DN, Dudemaine PL, Fomenky BE, Ibeagha-Awemu EM. Integration of miRNA weighted gene co-expression network and miRNA-mRNA co-expression analyses reveals potential regulatory functions of miRNAs in calf rumen development. Genomics. 2019; 111(4):849-59.
37. Xiao ZQ, Majumdar AP. Increased in vitro activation of EGFR by membrane-bound TGF-alpha from gastric and colonic mucosa of aged rats. Am J Physiol Gastrointest Liver Physiol. 2001; 281(1):G111-6.
38. Osaki LH, Figueiredo PM, Alvares EP, Gama P. EGFR is involved in control of gastric cell proliferation through activation of MAPK and Src signalling pathways in early-weaned rats. Cell Prolif. 2011; 44(2):174-82.
39. Xiao C, Hong H, Yu H, Yuan J, Guo C, Cao H, et al. MiR-340 affects gastric cancer cell proliferation, cycle, and apoptosis through regulating SOCS3/JAK-STAT signaling pathway. Immunopharmacol Immunotoxicol. 2018; 40(4):278-83.
40. Depeille P, Henricks LM, van de Ven RA, Lemmens E, Wang CY, Matli M, et al. RasGRP1 opposes proliferative EGFR-SOS1-Ras signals and restricts intestinal epithelial cell growth. Nat Cell Biol. 2015, 17(6):804-15.
41. Waseem T, Duxbury M, Ashley SW, Robinson MK. Ghrelin promotes intestinal epithelial cell proliferation through PI3K/Akt pathway and EGFR trans-activation both converging to ERK 1/2 phosphorylation. Peptides. 2014; 52:113-21.
42. Baldwin RLt, Connor EE. Rumen Function and Development. Vet Clin North Am Food Anim Pract. 2017; 33(3):427-39.
43. Greco G, Hagen F, Meissner S, Shen Z, Lu Z, Amasheh S, et al. Effect of individual SCFA on the epithelial barrier of sheep rumen under physiological and acidotic luminal pH conditions. J Anim Sci. 2018; 96(1):126-42.
44. Jing X, Wang W, Degen A, Guo Y, Kang J, Liu P, et al. Tibetan sheep have a high capacity to absorb and to regulate metabolism of SCFA in the rumen epithelium to adapt to low energy intake. Br J Nutr. 2020; 123(7):721-36.
45. Malmuthuge N, Liang G, Guan LL. Regulation of rumen development in neonatal ruminants through microbial metagenomes and host transcriptomes. Genome Biol. 2019; 20(1):172.
46. Xue M, Wang K, Wang A, Li R, Wang Y, Sun S, et al. MicroRNA Sequencing Reveals the Effect of Different Levels of Non-Fibrous Carbohydrate/Neutral Detergent Fiber on Rumen Development in Calves. Animals (Basel). 2019; 9(8):496.
47. Li Y, Carrillo JA, Ding Y, He Y, Zhao C, Liu J, et al. DNA methylation, microRNA expression profiles and their relationships with transcriptome in grass-fed and grain-fed Angus cattle rumen tissue. Plos One. 2019; 14(10):e0214559.
48. Raut A, Khanna A. Enhanced expression of hepatocyte-specific microRNAs in valproic acid mediated hepatic trans-differentiation of human umbilical cord derived mesenchymal stem cells. Exp Cell Res. 2016, 343(2):237-47.
49. Jung KH, Zhang J, Zhou C, Shen H, Gagea M, Rodriguez-Aguayo C, et al. Differentiation therapy for hepatocellular carcinoma: Multifaceted effects of miR-148a on tumor growth and phenotype and liver fibrosis. Hepatology. 2016; 63(3):864-79.
50. Song C, Yang J, Jiang R, Yang Z, Li H, Huang Y, et al. miR-148a-3p regulates proliferation and apoptosis of bovine muscle cells by targeting KLF6. J Cell Physiol. 2019; DOI: 10.1002/jcp.28232.
51. He H, Cai M, Zhu J, Xiao W, Liu B, Shi Y, et al. miR-148a-3p promotes rabbit preadipocyte differentiation by targeting PTEN. In Vitro Cell Dev Biol Anim. 2018; 54(3):241-49.
52. Mai M, Jin L, Tian S, Liu R, Huang W, Tang Q, et al. Deciphering the microRNA transcriptome of skeletal muscle during porcine development. PeerJ. 2016; 4:e1504.
53. Sharma M, Sharma S, Alawada A. Understanding the binding specificities of mRNA targets by the mammalian Quaking protein. Nucleic Acids Res. 2019; 47(20):10564-79.

54. Wu Y, Li Z, Yang M, Dai B, Hu F, Yang F, et al. MicroRNA-214 regulates smooth muscle cell differentiation from stem cells by targeting RNA-binding protein QKI. Oncotarget. 2017; 8(12):19866-78.
55. He Z, Yi J, Liu X, Chen J, Han S, Jin L, et al. MiR-143-3p functions as a tumor suppressor by regulating cell proliferation, invasion and epithelial–mesenchymal transition by targeting QKI-5 in esophageal squamous cell carcinoma. Mol Cancer. 2016; 15(1):51.
56. Iwata N, Ishikawa T, Okazaki S, Mogushi K, Baba H, Ishiguro M, et al. Clinical Significance of Methylation and Reduced Expression of the Quaking Gene in Colorectal Cancer. Anticancer Res. 2017; 37(2):489-98.
57. Li X, Wang L, Cao X, Zhou L, Xu C, Cui Y, et al. Casticin inhibits stemness of hepatocellular carcinoma cells via disrupting the reciprocal negative regulation between DNMT1 and miR-148a-3p. Toxicol Appl Pharmacol. 2020, 396:114998.
58. Long XR, He Y, Huang C, Li J. MicroRNA-148a is silenced by hypermethylation and interacts with DNA methyltransferase 1 in hepatocellular carcinogenesis. Int J Oncol. 2014; 44(6):1915-22.
59. Li Y, Chen F, Chu J, Wu C, Li Y, Li H, et al. miR-148-3p Inhibits Growth of Glioblastoma Targeting DNA Methyltransferase-1 (DNMT1). Oncol Res. 2019; 27(8):911-21.
60. Wang X, Liang Z, Xu X, Li J, Zhu Y, Meng S, Li S, Wang S, Xie B, Ji A et al: miR-148a-3p represses proliferation and EMT by establishing regulatory circuits between ERBB3/AKT2/c-myc and DNMT1 in bladder cancer. Cell Death Dis. 2016; 7(12):e2503.

Tables

Tabel 1: Information on high expression of miRNAs in the rumen of four different periods of goats

miRNAs	Sequences (5'-3')	E60 (TPM)			E135 (TPM)			D30 (TPM)		
		S01	S02	S03	S04	S05	S06	S07	S08	S09
chi-miR-143-3p	UGAGAUGAAGCACUGUAGCUCG	129899	108660	133032	282443	236491	248819	169226	283572	256290
chi-miR-148a-3p	UCAGUGCACUACAGAACUUUGU	49694	63518	61760	53323	57021	73459	162467	123649	134682
chi-miR-21-5p	UAGCUUAUCAGACUGAUGUUGAC	34325	42267	40250	36374	38253	35896	52698	67018	55942
chi-miR-26a-5p	UUCAAGUAAUCCAGGAUAGGCU	42298	29748	38171	37739	42639	38951	58680	50393	45517
chi-let-7f-5p	UGAGGUAGUAGAUUGUAUAGUU	48221	37487	48836	39702	48107	43888	42275	27161	34007
chi-let-7i-5p	UGAGGUAGUAGUUUGUGCUGUU	89489	59637	80713	48114	55336	54657	103139	72450	83736
chi-let-7g-5p	UGAGGUAGUAGUUUGUACAGUU	39837	27270	33591	25214	27819	25772	39747	26332	30420
chi-miR-10a-5p	UACCCUGUAGAUCCGAAUUUGU	39578	56845	25376	46805	49823	49493	16458	18478	18094
novel_miR_816	GUGAAAUGUUUAGGACCACUAG	7716.7	10842	5830.4	43032	51745	38204	25771	31989	23516
chi-miR-27b-3p	UUCACAGUGGCUAAGUUCUGC	22255	22535	26818	34768	35165	32999	22256	24188	22919
chi-miR-7-5p	UGGAAGACUAGUGAUUUUGUUGUU	40591	12547	37260	2969.5	3014.7	3654.1	5162.3	3850.8	2571.8
chi-miR-127-3p	UCGGAUCCGUCUGAGCUUGG	22242	33430	22459	10291	11179	11424	6808.4	9133.8	10262
chi-miR-99a-5p	AACCCGUAGAUCCGAUCUUGU	21044	23685	22251	21409	21531	23416	29878	23867	25090
chi-miR-1	UGGAAUGUAAAGAAGUAUGUAU	6661.5	24793	3678.9	12652	12841	10219	5476.6	6946.7	8300
chi-miR-145-5p	GUCCAGUUUUCCCAGGAAUCCCU	23695	6810.1	16205	27622	26221	23252	14500	18637	24478

Figures

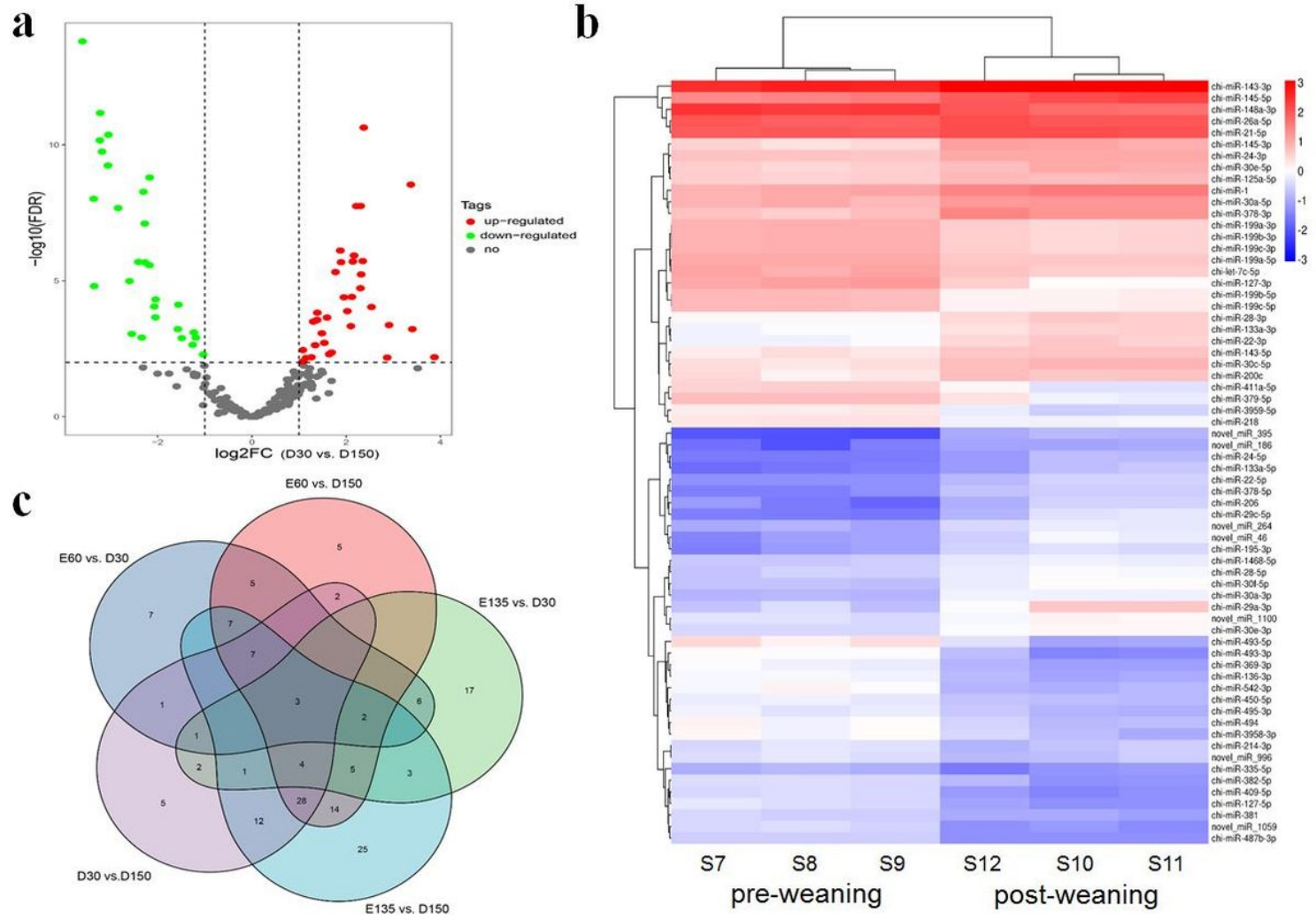

Figure 1

a Numbers of up-regulated and down-regulated DEMs in goat rumens at D30 and D150. b Hierarchical clustering analysis of DEMs. c Venn diagram showing the commonly and uniquely DEMs in different pairwise comparisons.

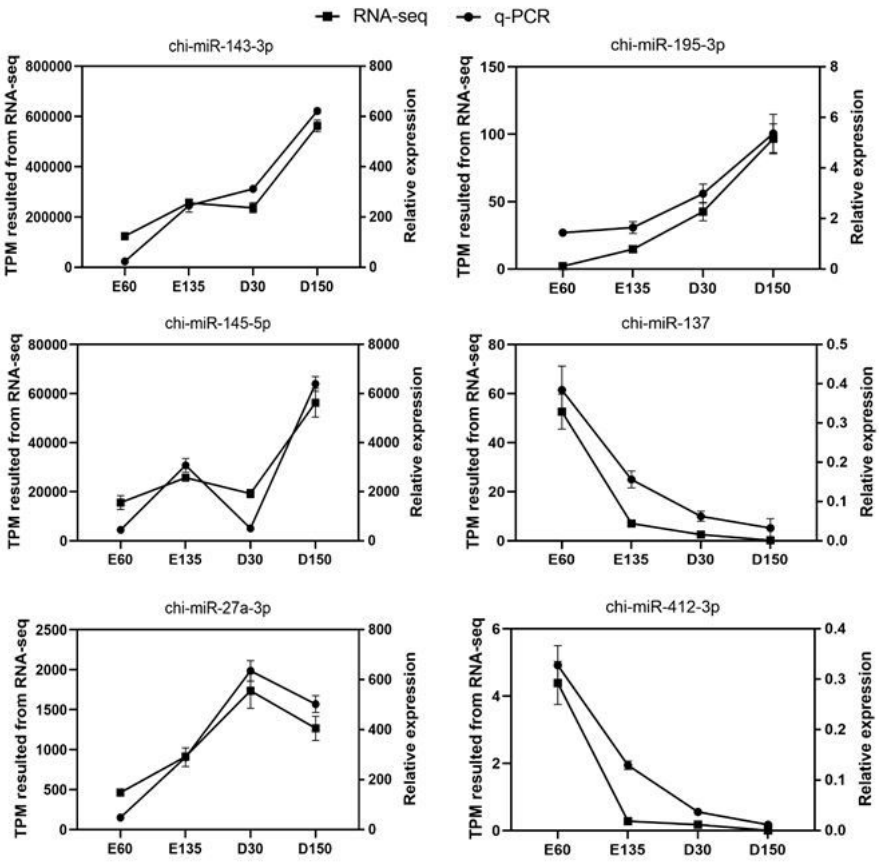

Figure 2

Validation of the six selected DEMs by qPCR.

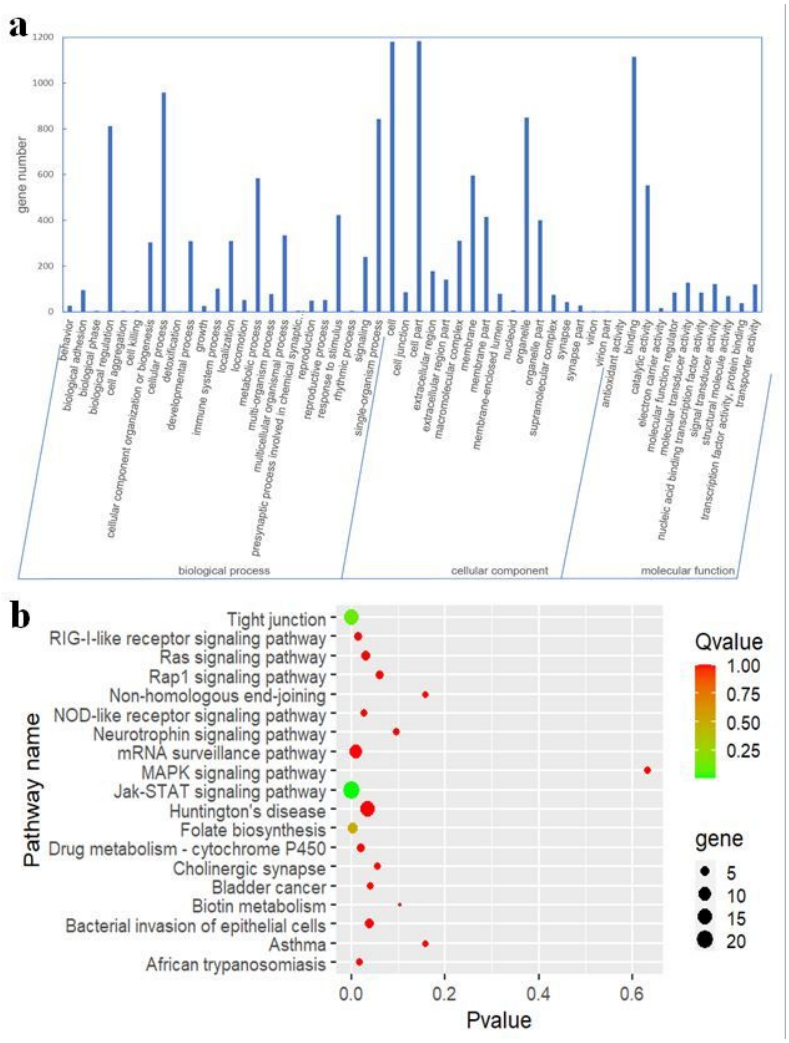

Figure 3

a GO functional classification of genes predicated from the DEMs. b Enrichment analysis of KEGG pathway in target genes of the DEMs.

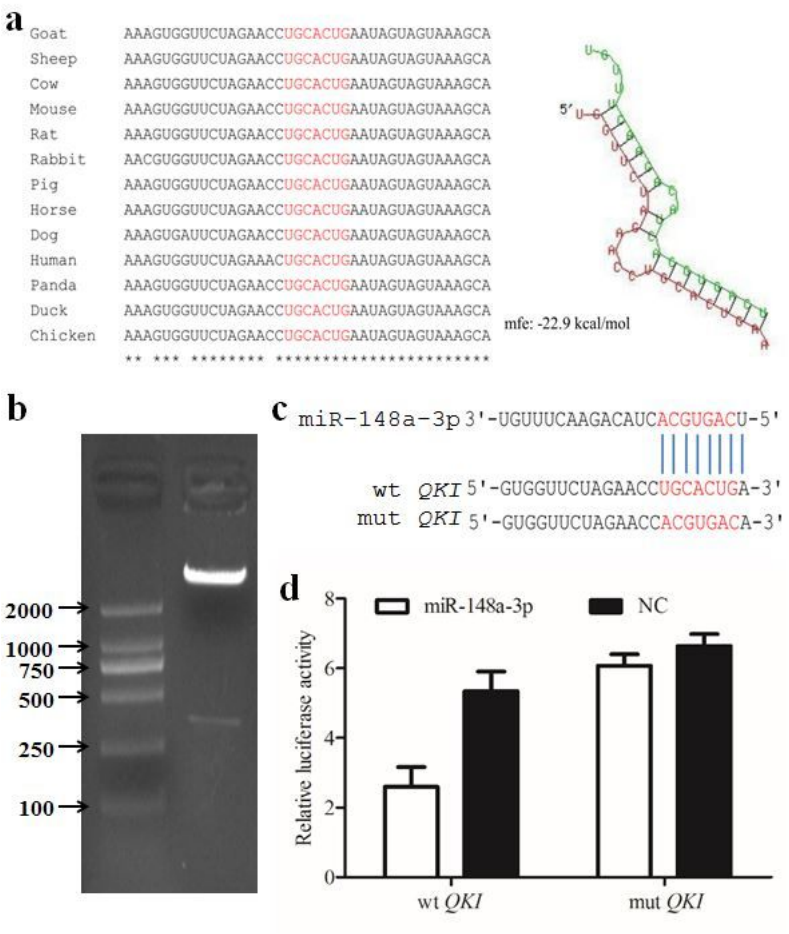

Figure 4

a Alignment of binding sites among different species and the predicted secondary structure of miR-148a-3p and targeting QKI. b Electrophoresis of the recombinant plasmid. c Base complementarity between miR-148a-30 and the 3'-UTR of QKI. d Luciferase reporter assay of HEK293T cells co-transfected with QKI wild-type or QKI mutant-type and miR-148a-3p mimics

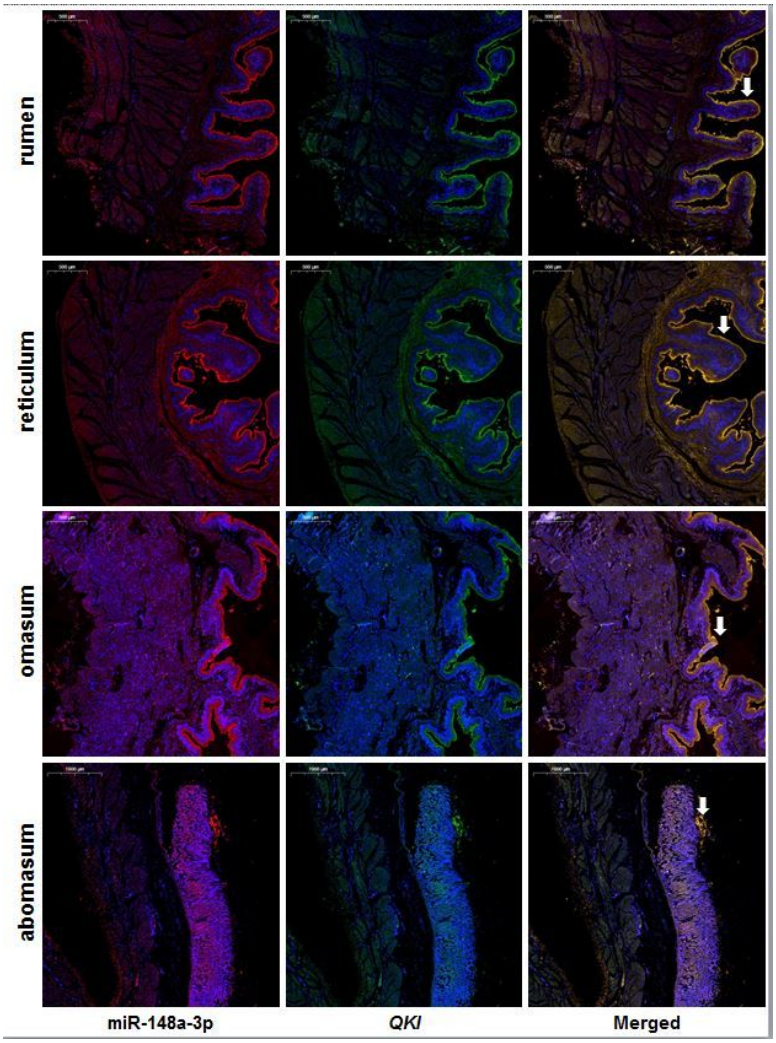

Figure 5

Co-location of miR-148a-3p and QKI in different stomach chambers. Bar. 500 μm. Arrows indicates the epithelial layer.

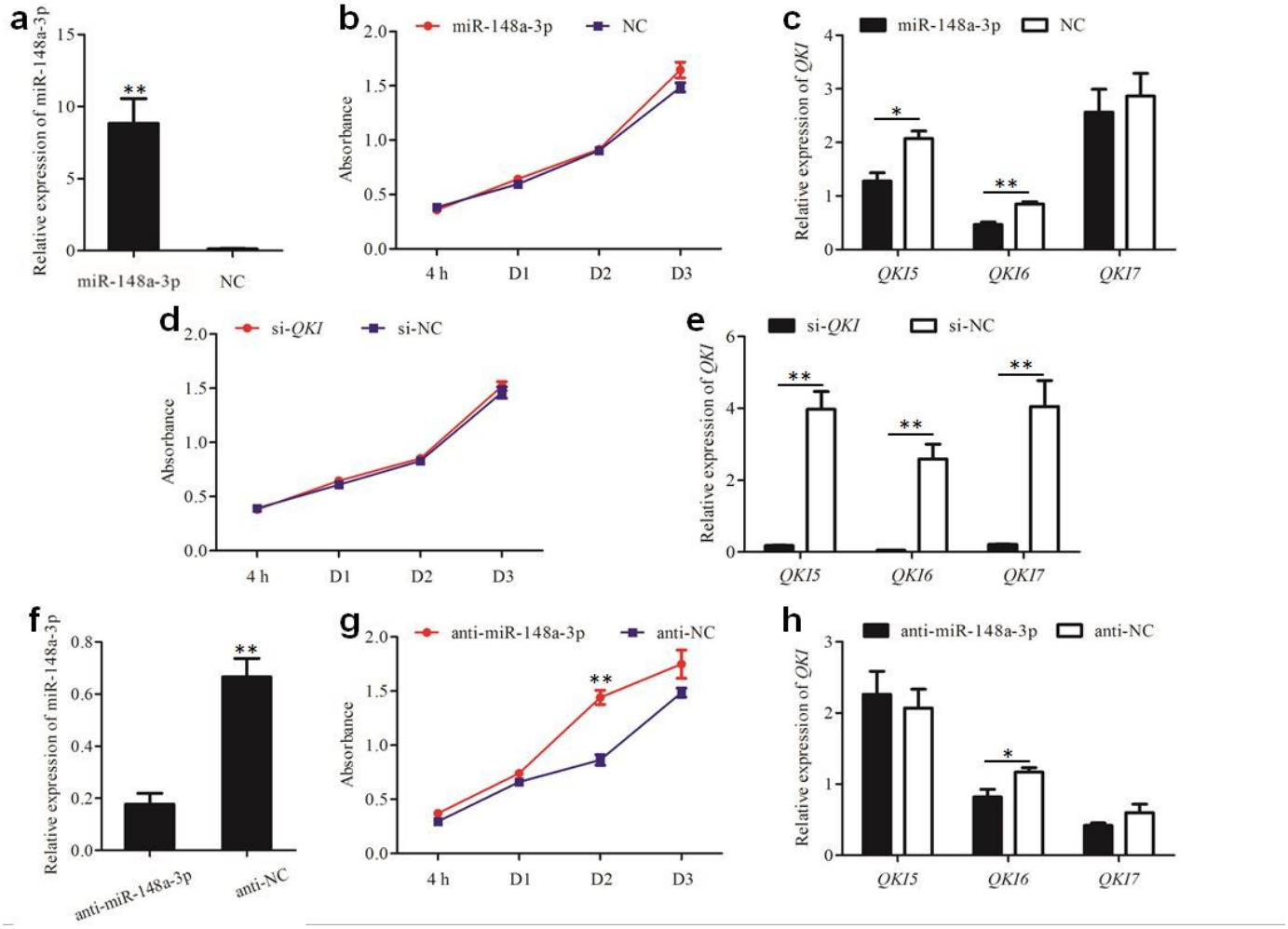

Figure 6

miR-148a-3p regulates cell proliferation of GES-1. a the efficiency of miR-148a-3p mimics transfection. b growth curve of GES-1 cells transfected with miR-148a-3p mimics. c relative expression of main isoforms of QKI after transfection with miR-148a-3p mimics. d growth curve of GES-1 cells transfected with QKI siRNA. e the efficiency of QKI siRNA transfection. f the efficiency of miR-148a-3p inhibitor transfection. g growth curve of GES-1 cells transfected with miR-148a-3p inhibitor. h relative expression of main isoforms of QKI after transfection with miR-148a-3p mimics.

Supplementary Files

This is a list of supplementary files associated with this preprint. Click to download.

- Additionalfile1TableS1.doc
- Additionalfile3TableS2.doc
- Additionalfile5TableS4.xls
- Additionalfile8TableS6.doc
- Additionalfile7TableS5.xls
- Additionalfile9TableS7.doc
- Additionalfile6FigureS2.ppt
- Additionalfile4TableS3.xls
- Additionalfile2FigureS1.ppt
- Additionalfile10FigureS3.ppt